Polish Society of Composite Materials
Polskie Towarzystwo Materiałów Kompozytowych

22: 1 (2022) 25-39

COMPOSITES THEORY AND PRACTICE
ISSN: 2084-6096
ISSN (online): 2299-128X

Marian Klasztorny*, Daniel B. Nycz

Institute of Technology, Jan Grodek State University in Sanok, ul. A. Mickiewicza 21, 38-500 Sanok, Poland
[a] At present: Professor Emeritus in Civil and Mechanical Engineering
**Corresponding author. E-mail: m.klasztorny@gmail.com*

Received (Otrzymano) 13.01.2022

MODELLING OF LINEAR ELASTICITY AND VISCOELASTICITY OF THERMOSETS AND UNIDIRECTIONAL GLASS FIBRE-REINFORCED THERMOSET-MATRIX COMPOSITES – PART 2: HOMOGENIZATION AND NUMERICAL ANALYSIS

The study continues the advanced analytical modelling of the linear elasticity and viscoelasticity of thermosets and unidirectional glass fibre-reinforced thermoset-matrix (UFRT) composites. The thermosets are isotropic materials with viscoelastic shear strains and elastic bulk strains, and the fibres are isotropic and elastic. The modified homogenization theory for UFRT composites, based on the selected tasks of the linear theory of elasticity, is developed. The modifications include a volumetrically equivalent cylindrical representative volume cell, solutions determined for an isotropic fibre based on the solutions for a monotropic (transversely isotropic) fibre, and certain modifications in the third task of the theory of elasticity. The viscoelastic constants of the thermoset are derived analytically and validated by fitting of the simulation and experimental shear strains on a logarithmic time scale in the unidirectional tension creep test. The viscoelastic constants of the UFRT composite are derived analytically and validated by fitting of the storage compliances corresponding to the new viscoelastic model and one obtained from the viscoelastic-elastic correspondence principle. The tension creep experiment is performed on the selected structural unsaturated polyester resin. Identification and validation are carried out for that thermoset and the corresponding UFRT composite with long E-glass fibres. All the modelling hypotheses are confirmed.

Keywords: **thermoset, unidirectional glass fibre-reinforced thermoset-matrix composite, rheological modelling, experimental tests, numerical analysis**

INTRODUCTION

The paper is a continuation of Part 1 (Ref. [1]) on the elastic and viscoelastic modelling of thermosets and unidirectional long glass fibre-reinforced thermoset-matrix (UFRT) composites. Part 1 consisted of the following sections: an introduction including the state of the art, research objectives, assumptions, modelling of the linear elasticity and viscoelasticity of thermosets, and modelling of the linear elasticity and viscoelasticity of UFRT composites. This paper (Part 2) includes the following sections: the modified homogenization of UFRT composites, a description of new numerical algorithms corresponding to the analytical solutions presented in Part 1, a description and analysis of the experimental and numerical tests on the representative materials (identification and validation).

New rheological models (coded H-R/H) for thermosets and UFRT composites, described by the smallest possible number of the material constants, were developed by Klasztorny and Nycz [1]. The generic function for viscoelastic shear/quasi-shear stresses in thermosets and UFRT composites is assumed as Mittag-Leffler fractional exponential function in an integral form. The H-R/H model of the thermoset is described by two elastic and three viscoelastic constants. The H-R/H model of the homogenized UFRT composite is described by five elastic and five viscoelastic constants.

The homogenization of a UFRT composite with monotropic fibres was formulated by Wilczynski and Lewinski [2, 3] and next developed by Klasztorny et al. [4]. The modified homogenization theory for UFRT composites, presented in this study includes the following modifications: a volumetrically equivalent cylindrical representative volume cell, solutions determined for an isotropic fibre based on the solutions for a monotropic (transversely isotropic) fibre, and certain modifications in the third task of the theory of elasticity.

The viscoelastic constants of a thermoset, relative to the H-R/H rheological model, will be derived analytically and validated by fitting of the simulation and experimental shear strains vs. time (in a logarithmic scale) corresponding to the unidirectional tension creep test. The viscoelastic constants of a UFRT composite will be derived analytically and validated by fitting of the storage compliances corresponding to the H-R/H viscoelastic model and one obtained from the viscoelastic-elastic correspondence principle (VECP). The tension

creep experiment was performed on the selected structural unsaturated polyester resin. The identification and validation were carried out for that thermoset and the corresponding UFRT composite with long E-glass fibres. Selected final formulas determined in Ref. [1], used in this paper, are summarized in Appendix A.

The main research objectives are as follows:

- to develop a modified homogenization theory for UFRT composites;
- to develop an analytical algorithm in order to determine the viscoelastic constants of a UFRT composite using the viscoelastic-elastic correspondence principle;
- to determine the elasticity and viscoelasticity constants of the exemplary thermoset, describing the H-R/H model at RT, on the basis of the unidirectional tension creep test;
- to determine the elastic and viscoelastic constants of an exemplary UFRT composite, describing the H-R/H model at RT, on the basis of the modified homogenization theory and the viscoelastic-elastic correspondence principle.

The following assumptions are made (Ref. [1]):

- a new non-aging material fully relaxed after the curing and post-curing processes (free of residual stresses);
- quasi-static long-term isothermal viscoelastic processes;
- normal conditions;
- low levels of stresses in the thermoset matrix providing reversibility of the elastic and viscoelastic processes;
- long continuous rectilinear fibres arranged unidirectionally and uniformly in the matrix in a hexagonal scheme;
- a cylindrical representative volume cell (RVC) equivalent in volume to the true hexagonal cell;
- a linear viscoelastic isotropic thermoset described by the H-R/H (shear/bulk) rheological model;
- linear elastic isotropic fibres with an identical circular cross section;
- a linear viscoelastic monotropic composite after homogenization.

HOMOGENIZATION OF UFRT COMPOSITES

This Section presents a modified homogenization theory of a UFRT composite. The base publication is Ref. [4]. The modifications include:

- determination of analytical solutions of theory of elasticity tasks for an isotropic fibre based on the solutions for a monotropic (transversely isotropic) fibre;
- use of the arithmetic mean of two results to determine compliance S_{s4} in the third task of the theory of elasticity.

Note, a real hexagonal representative volume cell (RVC) is replaced with a cylindrical RVC without changing the value of the parameter f.

The purpose of homogenizing (micro-modelling) a UFRT composite, meeting the assumptions listed in Ref. [1], is to determine the effective elasticity constants (EECs) of the equivalent homogeneous monotropic continuum, i.e. $E_1, E_2, \nu_{21}, \nu_{32}, G_{12}$. These constants will be determined analytically on the basis of the solutions of selected tasks of the classic theory of elasticity concerning a RVC. The EECs are expressed in terms of the elastic constants of the thermoset matrix (E, ν), the elastic constants of the glass fibre (E_f – Young's modulus, ν_f – Poisson's ratio), and fibre volume fraction f. The shear and bulk modules for a thermoset are defined in Ref. [1], and for a fibre

$$G_f = E_f/2(1+\nu_f) \ , \ \ B_f = E_f/3(1-2\nu_f) \tag{1}$$

The RVC is assumed as a cylinder composed of a circular central disk with radius a and thickness $2h$ and a ring disk with outer radius b and thickness $2h$, as shown in Figure 1. The RVC is equivalent volumetrically to the real hexagonal cell, hence $a = b\sqrt{f}$. The homogenized RVC is a circular disk with radius b and thickness $2h$. The RVC is described in the $x_1 r\varphi$ cylindrical coordinate system corresponding to the $x_1 x_2 x_3$ Cartesian coordinate system. The RVC is a $2h$ thick section of an infinitely long two-phase cylinder.

The elastic directional compliances of a thermoset matrix are expressed in terms of the elastic shear/bulk compliances of the matrix, i.e. [1]

$$S_{11,m} = (2S_s + S_b)/3 \ , \ \ S_{12,m} = (S_b - S_s)/3 \tag{2}$$

where (see Eqns. $(A.3)_{6\text{-}8}$, $(A.5)_4$)

$$S_{11,m} = 1/E, \ \ S_{12,m} = -\nu/E, \ \ S_s = 1/2G, \ \ S_b = 1/3B \tag{3}$$

By multiplying Eqns. (2, 3) by E_f, we get dimensionless equations, i.e.

$$s_{11} = (2s_s + s_b)/3 \ , \ \ s_{12} = (s_b - s_s)/3 \tag{4}$$

where

$$s_{11} = E_f/E \ , \ \ s_{12} = -\nu E_f/E \ , \ \ s_s = E_f/2G \ , \ \ s_b = E_f/3B \tag{5}$$

In further considerations, quantities $S_{11,h}, S_{22,h}, S_{12,h}, S_{23,h}, S_{s4,h}, S_{s5,h}$ are elements of elastic compliance matrices $\mathbf{S}, \{\mathbf{S}\}$ (Ref. [1]) corresponding to the normal/shear strains for the homogeneous monotropic material, respectively. Compliances

$$S_{2,h} = (1-\nu_{32})/E_2 \ , \ \ S_{s4,h} = (1+\nu_{32})/E_2 \tag{6}$$

allow two compliances of the homogenized composite to be determined, i.e.

$$S_{22,h} = (S_{2,h} + S_{s4,h})/2 \ , \ \ S_{23,h} = (S_{2,h} - S_{s4,h})/2 \tag{7}$$

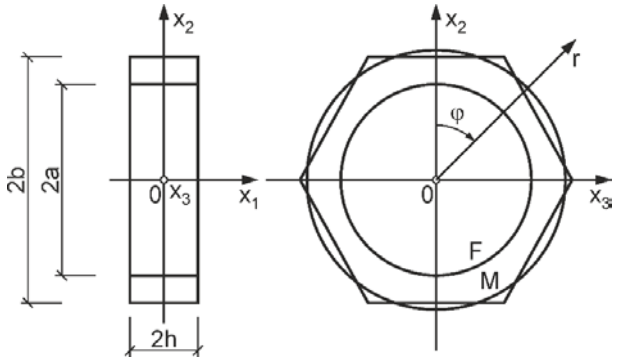

Fig. 1. Two-phase RVC on background of real hexagonal cell

The following designations corresponding to the RVC are introduced:
A, B, C, D – integration constants corresponding to the polymer matrix,
$A_\mathrm{f}, B_\mathrm{f}, C_\mathrm{f}$ – integration constants corresponding to the glass fibre,
u_1, u, v – displacement components in cylindrical coordinates, corresponding to the RVC polymer matrix,
$u_{1\mathrm{f}}, u_\mathrm{f}, v_\mathrm{f}$ – displacement components in cylindrical coordinates, corresponding to the RVC fibre,
$u_{1\mathrm{c}}, u_\mathrm{c}, v_\mathrm{c}$ – displacement components in cylindrical coordinates, corresponding to the RVC homogenized composite,
$\sigma_1, \sigma_\mathrm{r}, \sigma_\varphi, \tau_{\mathrm{r}\varphi}, \tau_{1\mathrm{r}}$ – stress components in cylindrical coordinates, corresponding to the RVC polymer matrix,
$\sigma_{1\mathrm{f}}, \sigma_{\mathrm{rf}}, \sigma_{\varphi\mathrm{f}}, \tau_{\mathrm{r}\varphi\mathrm{f}}, \tau_{1\mathrm{rf}}$ – stress components in cylindrical coordinates, corresponding to the RVC fibre,
$\sigma_{1\mathrm{c}}, \sigma_{\mathrm{rc}}, \sigma_{\varphi\mathrm{c}}, \tau_{\mathrm{r}\varphi\mathrm{c}}, \tau_{1\mathrm{rc}}$ – stress components in cylindrical coordinates, corresponding to the RVC homogenized composite,
σ_0, τ_0 – maximum normal/shear stress,
$p_{11}, p_{22}, p_{12}, p_{21}, p_1, p_2, p_3, p_4, p$ – auxiliary coefficients in the analytical solutions of theory of elasticity tasks.

The displacement and stress components in the $x_1 r\varphi$ cylindrical coordinate system are shown in Figure 2.

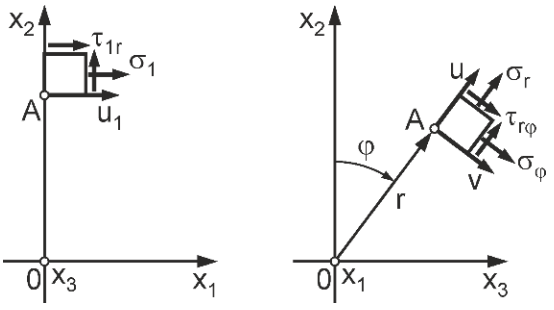

Fig. 2. Displacement and stress components in $x_1 r\varphi$ cylindrical coordinate system

The following tasks of the classic theory of elasticity were chosen (Refs. [2-4]):
1) longitudinal uniform tension in the x_1 direction;
2) axially-symmetric transverse tension in the $x_2 x_3$ plane;
3) transverse shear in the $x_2 x_3$ plane;
4) longitudinal shear in the $x_1 x_2$ plane.

Consider the first task illustrated in Figure 3. According to the true response of the UFRT composite, the longitudinal elongation of both phases $u_1 = \mathrm{const}$ (Fig. 3a). It results in a normal stress distribution before homogenization $\sigma_1 = \mathrm{const}$, $\sigma_{1\mathrm{f}} = \mathrm{const}$ and after homogenization $\sigma_0 = \mathrm{const}$, as shown in Figure 3b, c.

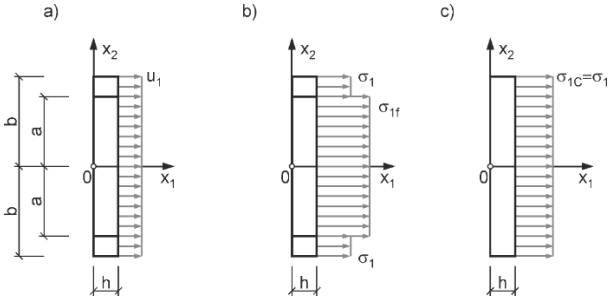

Fig. 3. First task in homogenization theory of UFRT composite

The general solutions in the first task have the following form:
- stresses and displacements in the fibre $(0 \le r \le a)$:

$$\sigma_{\mathrm{rf}} = 2C_\mathrm{f}\ ,\ \ \sigma_{\varphi\mathrm{f}} = 2C_\mathrm{f}$$
$$u_\mathrm{f}(r) = r[2(1-\nu_\mathrm{f})C_\mathrm{f} - \nu_\mathrm{f}\sigma_{1\mathrm{f}}]/E_\mathrm{f}\ ,$$
$$u_{1\mathrm{f}}(x_1) = x_1(\sigma_{1\mathrm{f}} - 4\nu_\mathrm{f}C_\mathrm{f})/E_\mathrm{f} \qquad (8)$$

- stresses and displacements in the matrix $(a \le r \le b)$:

$$\sigma_r(r) = A/r^2 + 2C\ ,\ \ \sigma_\varphi(r) = -A/r^2 + 2C$$
$$u_r(r) = r[-\nu\sigma_1 - (1+\nu)\,A/r^2 + 2(1-\nu)C]/E\ ,$$
$$u_1(x_1) = x_1(\sigma_1 - 4\nu C)/E \qquad (9)$$

- stresses and displacements in the homogenized RVC $(0 \le r \le b)$:

$$\sigma_{rc} = 0\ ,\ \ \sigma_{\varphi c} = 0$$
$$u_\mathrm{c}(r) = -r\nu_{21}\sigma_0/E_1\ ,\ \ u_{1\mathrm{c}}(x_1) = x_1\sigma_0/E_1 \qquad (10)$$

The boundary conditions in the stresses have the form:

$$\sigma_{1\mathrm{f}}\,f + \sigma_1(1-f) = \sigma_0\ ,\ \ \sigma_r(b) = 0 \qquad (11)$$

The continuity conditions have the form

$$\sigma_{\mathrm{rf}}(a) = \sigma_r(a)\ ,\ \ u_\mathrm{f}(a) = u(a)\ ,\ \ u_{1\mathrm{f}}(h) = u_1(h) \qquad (12)$$

The compatibility conditions in the displacements have the form

$$u(b) = u_\mathrm{c}(b)\ ,\ \ u_1(h) = u_{1\mathrm{c}}(h) \qquad (13)$$

Equations (11)-(13) form a system of 7 linear algebraic equations with unknowns $\sigma_{1\mathrm{f}}, \sigma_1, C_\mathrm{f}, A, C, S_{11,\mathrm{h}}, S_{12,\mathrm{h}}$. The results in terms of the elastic compliances of the homogenized composite are as follows:

$$S_{11,\mathrm{h}} = (p_2 s_{11} - 2p_1 s_{12})/p/E_\mathrm{f}\ ,$$
$$S_{12,\mathrm{h}} = (p_2 s_{12} - 2p_1 s_{11})/p/E_\mathrm{f} \qquad (14)$$

where

$$p_1 = p_{22}\nu_\mathrm{f} - p_{12}\ ,\ \ p_2 = p_{11} - p_{21}\nu_\mathrm{f}\ ,$$
$$p = p_{11}p_{22} - p_{12}p_{21}$$
$$p_{11} = (1-f)(1-\nu_\mathrm{f}) + (1+f)s_{11} - (1-f)s_{12}\ ,$$
$$p_{22} = 1 + f(s_{11} - 1)$$
$$p_{12} = (1-f)\nu_\mathrm{f} - fs_{12}\ ,\ \ p_{21} = 2(1-f)\nu_\mathrm{f} - 2fs_{12} \tag{15}$$

Consider the second task illustrated in Figure 4. According to the true response of the UFRT composite, the longitudinal contraction (negative elongation) of both phases $u_1 = \mathrm{const}$ as shown in Figure 4b. It results in a normal stress distribution before homogenization $\sigma_1 = \mathrm{const},\ \sigma_{1\mathrm{f}} = \mathrm{const}$ (Fig. 4c) and after homogenization $\sigma_{1\mathrm{c}} = 0$.

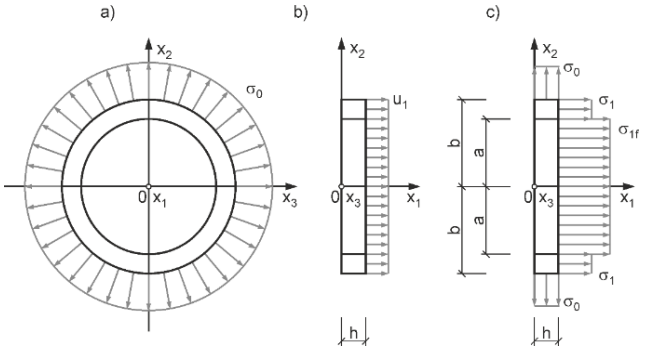

Fig. 4. Second task in homogenization theory of UFRT composite

The stresses and displacements in the fibre and the matrix are described by Eqns. (8, 9), whereas for the homogenized RVC the following formulae are obtained $(0 \le r \le b)$:

$$\sigma_{r\mathrm{c}} = \sigma_0\ ,\ \ \sigma_{\varphi\mathrm{c}} = \sigma_0$$
$$u_\mathrm{c}(r) = r(1-\nu_{32})\sigma_0/E_2\ ,\ \ u_{1\mathrm{c}}(x_1) = -2\,x_1\nu_{21}\sigma_0/E_1 \tag{16}$$

The boundary conditions in the stresses have the form:

$$\sigma_{1\mathrm{f}}\,f + \sigma_1(1-f) = 0\ ,\ \ \sigma_r(b) = \sigma_0 \tag{17}$$

The continuity and compatibility conditions are described by Eqns. (12, 13). Equations (12, 13, 17) form a system of 7 linear algebraic equations with unknowns $\sigma_{1\mathrm{f}}, \sigma_1, C_\mathrm{f}, A, C, S_{2,\mathrm{h}}, S_{12,\mathrm{h}}$. The results in terms of the elastic compliances of the homogenized composite are as follows:

$$S_{2,\mathrm{h}} = [s_{11} + s_{12} + (p_4 s_{12} - 2p_3 s_{11})/p]/E_\mathrm{f}$$
$$S_{12,\mathrm{h}} = [s_{12} + (p_4 s_{11}/2 - p_3 s_{12})/p]/E_\mathrm{f} \tag{18}$$

where

$$p_3 = p_{22}\big[(1-\nu)s_{11} - (1-\nu_f)\big]f + 2p_{12}(\nu_\mathrm{f} + s_{12})f$$
$$p_4 = -2p_{11}(\nu_\mathrm{f} + s_{12})f - p_{21}\big[(1-\nu)s_{11} - (1-\nu_f)\big]f \tag{19}$$

Coefficients $p_{11}, p_{22}, p_{12}, p_{21}, p$ are defined in Eqns. $(15)_{3\text{-}7}$. It can be shown that equations $(14)_2$, $(18)_2$ are equivalent.

The third task is related to the RVC loaded transversely on the boundary $r = b$ with the following stresses:

$$\sigma_r(b,\varphi) = \sigma_0 \cos 2\varphi\ ,\ \ \tau_{r\varphi}(b,\varphi) = -\sigma_0 \sin 2\varphi \tag{20}$$

as shown in Figure 5. According to the true response of the UFRT composite, this load induces a planar strain state $(\varepsilon_1 = 0)$. It results in non-uniform normal stresses before and after homogenization.

The general solutions in the third task have the following form:

- stresses and displacements in the fibre $(0 \le r \le a)$:

$$\sigma_{r\mathrm{f}}(\varphi) = -2A_\mathrm{f}\cos 2\varphi\ ,\ \ \sigma_{\varphi\mathrm{f}}(r,\varphi) = 2(A_\mathrm{f} + 6B_\mathrm{f}\,r^2)\cos 2\varphi$$
$$\tau_{r\varphi\mathrm{f}}(r,\varphi) = 2(A_\mathrm{f} + 3B_\mathrm{f}\,r^2)\sin 2\varphi$$
$$u_\mathrm{f}(r,\varphi) = -2r[(1+\nu_\mathrm{f})A_\mathrm{f} + 2\nu_\mathrm{f}(1+\nu_\mathrm{f})B_\mathrm{f}\,r^2]/E_\mathrm{f}\cdot\cos 2\varphi$$
$$v_\mathrm{f}(r,\varphi) = 2r\big[(1+\nu_\mathrm{f})A_\mathrm{f} + \big(3+\nu_\mathrm{f} - 2\nu_\mathrm{f}^2\big)B_\mathrm{f}\,r^2\big]/E_\mathrm{f}\cdot\sin 2\varphi \tag{21}$$

- stresses and displacements in the matrix $(a \le r \le b)$:

$$\sigma_r(r,\varphi) = -2(A + 3C/r^4 + 2D/r^2)\cos 2\varphi$$
$$\sigma_\varphi(r,\varphi) = 2(A + 6Br^2 + 3C/r^4)\cos 2\varphi$$
$$\tau_{r\varphi}(r,\varphi) = 2(A + 3Br^2 - 3C/r^4 - D/r^2)\sin 2\varphi$$
$$u(r,\varphi) = -2r(1+\nu)[A + 2\nu Br^2 - C/r^4 - 2(1-\nu)\,D/r^2]/E\cdot\cos 2\varphi$$
$$v(r,\varphi) = 2r[(1+\nu)A + (3+\nu-2\nu^2)B\,r^2 + $$
$$+(1+\nu)\,C/r^4 - (1-\nu-2\nu^2)\,D/r^2]/E\cdot\sin 2\varphi \tag{22}$$

- stresses and displacements in the homogenized RVC $(0 \le r \le b)$:

$$\sigma_{r\mathrm{c}}(\varphi) = \sigma_0\cos 2\varphi\ ,\ \ \sigma_{\varphi\mathrm{c}}(\varphi) = -\sigma_0\cos 2\varphi\ ,$$
$$\tau_{r\varphi\mathrm{c}}(\varphi) = -\sigma_0\sin 2\varphi$$
$$u_\mathrm{c}(r,\varphi) = r(1+\nu_{32})\sigma_0/E_2\cdot\cos 2\varphi \tag{23}$$
$$v_\mathrm{c}(r,\varphi) = -r(1+\nu_{32})\sigma_0/E_2\cdot\sin 2\varphi$$

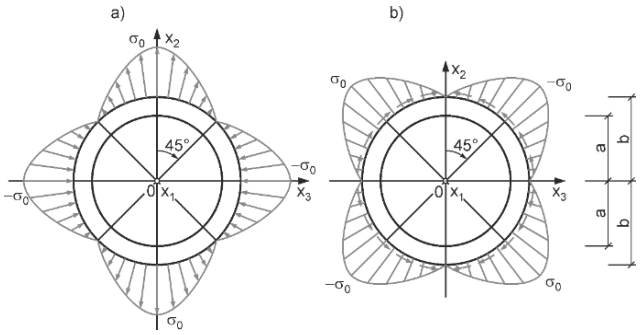

Fig. 5. Third task in homogenization theory of UFRT composite

The boundary conditions in the stresses are described by Eqns. (20). The continuity conditions have the form:

$$\sigma_{r\mathrm{f}}(a,\varphi) = \sigma_r(a,\varphi)\ ,\ \ \tau_{r\varphi\mathrm{f}}(a,\varphi) = \tau_{r\varphi}(a,\varphi)$$
$$u_\mathrm{f}(a,\varphi) = u(a,\varphi)\ ,\ \ v_\mathrm{f}(a,\varphi) = v(a,\varphi) \tag{24}$$

The compatibility condition has the form:

- radial direction

$$u(b,\varphi) = u_\mathrm{c}(b,\varphi) \tag{25}$$

- circumferential direction

$$v(b,\varphi) = v_\mathrm{c}(b,\varphi) \tag{26}$$

Equations (20, 24) form a system of six linear algebraic equations with unknowns $A_\mathrm{f}, B_\mathrm{f}, A, B, C, D$. Compliance $S_{\mathrm{s4,h}} = S_{\mathrm{s}4u}$ can be determined from Eqn. (25), and compliance $S_{\mathrm{s4,h}} = S_{\mathrm{s}4v}$ – from Eqn. (26). In further calculations, the arithmetic mean of these two predictions was adopted, i.e.

$$S_{\mathrm{s4,h}} = (S_{\mathrm{s}4u} + S_{\mathrm{s}4v})/2 = [1 + 2(1-\nu)\,p_1/p](s_{11} - s_{12})/E_\mathrm{f} \tag{27}$$

where

$$\begin{gathered} p_1 = [1 + \nu_\mathrm{f} - (1+\nu)s_{11}](p_{11} - p_{21}) \ , \ p = p_{11}p_{22} - p_{12}p_{21} \\ p_{11} = (1+\nu_\mathrm{f})[3(1/f^2 - 1) + 4\nu_\mathrm{f}\,(f - 1/f^2)] + \\ (1+\nu)(3 - 4\nu f + 1/f^2)s_{11} \\ p_{22} = 2(1+\nu_\mathrm{f})(1/f - 1) + [3 + \nu_\mathrm{f}(1 - 2\nu_\mathrm{f})](f - 1/f) + \\ +[2(1+\nu) - (3 + \nu - 2\nu^2)f + (1 - \nu - 2\nu^2)/f]s_{11} \\ p_{12} = 2(1+\nu_\mathrm{f})[(1/f - 1) + \nu_\mathrm{f}(f - 1/f)] + \\ 2(1+\nu)[1 - \nu f + (1-\nu)/f]s_{11} \\ p_{21} = 3(1+\nu_\mathrm{f})(1/f^2 - 1) + 2[3 + \nu_\mathrm{f}(1 - 2\nu_\mathrm{f})](f - 1/f^2) + \\ +[3(1+\nu) - 2(3 + \nu - 2\nu^2)f - (1+\nu)/f^2]s_{11} \end{gathered} \tag{28}$$

The fourth task is related to the RVC loaded tangentially in the longitudinal direction, on boundary $r = b$, by the following shear stress:

$$\tau_{1r}(b,\varphi) = \tau_0 \cos\varphi \tag{29}$$

as illustrated in Figure 6. According to the true response of the UFRT composite, the loading (29) induces pure longitudinal shear.

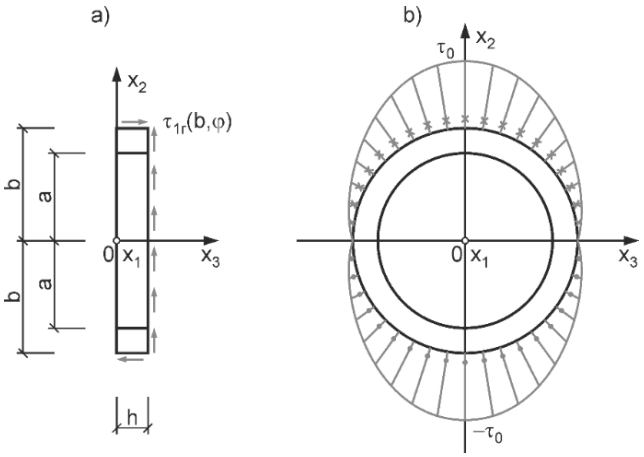

Fig. 6. Fourth task in homogenization theory of UFRT composite

The general solutions in the fourth task have the form

- stresses and displacements in the fibre $(0 \le r \le a)$:

$$\tau_{1\mathrm{rf}}(\varphi) = G_\mathrm{f} A_\mathrm{f} \cos\varphi \ , \ u_{1\mathrm{f}}(r,\varphi) = A_\mathrm{f}\, r \cos\varphi \tag{30}$$

- stresses and displacements in the matrix $(a \le r \le b)$:

$$\begin{gathered} \tau_{1r}(r,\varphi) = G(A - B/r^2)\cos\varphi \ , \\ u_1(r,\varphi) = r(A + B/r^2)\cos\varphi \end{gathered} \tag{31}$$

- stresses and displacements in the homogenized RVC $(0 \le r \le b)$:

$$\tau_{1\mathrm{rc}}(\varphi) = \tau_0 \cos\varphi \ , \ u_{1\mathrm{c}}(r,\varphi) = \tau_0\, r \cos\varphi / G_{12} \tag{32}$$

The boundary condition in the stress takes the form of Eqn. (29). The continuity conditions have the form

$$\tau_{1\mathrm{rf}}(\varphi) = \tau_{1r}(a,\varphi) \ , \ u_{1\mathrm{f}}(a,\varphi) = u_1(a,\varphi) \tag{33}$$

The compatibility condition has the form

$$u_1(b,\varphi) = u_{1\mathrm{c}}(b,\varphi) \tag{34}$$

Equations (29, 33, 34) form a system of four linear algebraic equations with $A_\mathrm{f}, A, B, S_{\mathrm{s5,h}}$ unknowns. The solution of these equations in terms of elastic compliance $S_{\mathrm{s5,h}}$ has the form

$$\begin{gathered} S_{\mathrm{s5,h}} = \\ s_\mathrm{s}[1 + f + s_\mathrm{s}(1-f)/(1+\nu_\mathrm{f})]/[1 - f + s_\mathrm{s}(1+f)/(1+\nu_\mathrm{f})]/E_\mathrm{f} \end{gathered} \tag{35}$$

The elastic compliances of composite UFRT, i.e. $S_{11}, S_{22}, S_{12}, S_{23}, S_{\mathrm{s}4}, S_{\mathrm{s}5}$, are defined by Eqns. (A.14)$_{3\text{-}8}$. As a result of composite homogenization, elastic compliances $S_{11,\mathrm{h}}, S_{12,\mathrm{h}}, S_{2,\mathrm{h}}, S_{\mathrm{s4,h}}, S_{\mathrm{s5,h}}$, defined by Eqns. (14, 18, 27, 35) were obtained. Compliances $S_{22,\mathrm{h}}, S_{23,\mathrm{h}}$ are calculated by means of Eqns. (7). From relations

$$\begin{gathered} S_{11} = S_{11,\mathrm{h}} \ , \ S_{22} = S_{22,\mathrm{h}} \ , \ S_{12} = S_{12,\mathrm{h}} \ , \\ S_{23} = S_{23,\mathrm{h}} \ , \ S_{\mathrm{s}5} = S_{\mathrm{s5,h}} \end{gathered} \tag{36}$$

the effective elastic constants of composite UFRT shall be determined, i.e.

$$\begin{gathered} E_1 = 1/S_{11,\mathrm{h}} \ , \ E_2 = 1/S_{22,\mathrm{h}} \ , \ \nu_{21} = -E_1 S_{12,\mathrm{h}} \ , \\ \nu_{32} = -E_2 S_{23,\mathrm{h}}, \ G_{12} = 1/2S_{\mathrm{s5,h}} \end{gathered} \tag{37}$$

A validation test of the homogenization theory was performed on an exemplary unidirectional E-glass fibre-reinforced vinylester-matrix composite. According to the producers' specifications, the elasticity constants of the components are: $E = 3.60$ MPa, $\nu = 0.35$, $E_f = $ $= 70.0$ MPa, $\nu_f = 0.20$. The laminate plate reinforced with a set of unidirectional glass fabrics was manufactured in 2014 using hand lay-up technology with fibre volume fraction $f = 0.29$.

TABLE 1. **Experimental and predicted values of elastic constants of exemplary homogenized UFRT composite along with relative deviation δ of predicted values**

	E_1 [GPa]	E_2 [GPa]	ν_{21}	ν_{32}	G_{12} [GPa]
Experiment	22.4	6.05	0.28	0.47	2.24
Prediction	22.9	5.80	0.30	0.50	2.29
δ [%]	2.2	-3.3	7.1	6.4	2.2

Experimental identification of the elastic constants of the UFRT composite was conducted in 2014 under normal conditions according to standard specifications [5-9]. The tensile, compression and shear tests were performed in 2014. The experiments and processing of the registered data are reported by Klasztorny et al. [10].

The experimental and predicted values of the independent elastic constants of the homogenized UFRT

composite are displayed in Table 1. The results confirm the technical acceptability of the modified homogenization theory.

NUMERICAL ALGORITHMS

Numerical integration

Function $L(u), 0 < r < 1$, defining the fractional exponential function in an integral form, is a continuous intermediate function between Dirac functions $\delta(u = 1)$ for $r = 1$ and $\delta(u = 0)$ for $r = 0$, and contains a singularity at point $u = 0$ (Eqn. $(A.5)_3$).

Consider an integral of the general form

$$J = \int_0^\infty f(u)\, du \tag{38}$$

in which the subintegral function $f(u)$ contains factor $L(u)$. The integral described by Eqn. (38) can be calculated numerically using a high-rank Gauss-Legendre quadrature. We perform a double shift of the variable

$$u = (1 - v)/v\ ,\ \ v = (1 + x)/2 \tag{39}$$

and transform Eqn. (38) to the form

$$J = 2\int_{-1}^{1} f(u)\,(1 + x)^{-2} dx\ ,\ \ u = (1 - x)/(1 + x) \tag{40}$$

Integration using the *n*-point Gauss-Legendre quadrature gives the result (Ref. [11])

$$J \approx 2\sum_{k=1}^{n} w_k f(u_k)\,(1 + x_k)^{-2}\ ,\ \ u_k = (1 - x_k)/(1 + x_k) \tag{41}$$

Quantities $w_k, x_k, k = 1, 2, \ldots, n$ are the weights and nodes of the *n*-point quadrature. Each subintegral function is approximated with a $(2n + 1)$th degree polynomial.

Formula (41) is used for integrals occurring in functions $T_c\,\Phi(\tau), \varphi(\tau)$, whereby $\tau = t/T_c$, $u^r = = \exp(r \ln u)$. In the case $f(u) = L(u)$ we obtain control condition $J = 1$ (Eqn. $(A.7)_2$).

Tension creep test on thermoset

The stress-controlled tension creep test on a thermoset in direction x_1 consists of two phases (Fig. 7). Phase 1 is elastic; stress $\sigma_1(t)$ increases quasi-linearly in interval $[0, \sigma_{1,0}]$ at a high stress rate, longitudinal strain $\varepsilon_1(t)$ increases quasi-linearly in interval $[0, \varepsilon_{1,0}]$, and transverse strains $\varepsilon_2(t) = \varepsilon_3(t)$ decrease quasi-linearly in interval $[0, \varepsilon_{2,0}]$, with $\varepsilon_{2,0} < 0$. Phase 1 is used to determine the elastic constants of the thermoset from the classical equations

$$E = \Delta\sigma_1/\Delta\varepsilon_1\ ,\ \ \nu = -\Delta\varepsilon_2/\Delta\varepsilon_1 \tag{42}$$

where $\Delta\varepsilon_2 < 0$. The use of stress and strain increments in the second part of Phase 1 allows elimination of measurement errors at the beginning of Phase 1. The appropriate level of stress $\sigma_{1,0}$ is to ensure the reversibility of deformations at creep. The shear and bulk constants G, B, S_s, S_b are calculated according to Eqns. (A.1), $(A.3)_8$, $(A.5)_4$.

In Phase 2, the sample is subjected to creep at a constant stress $\sigma_{1,0}$ in time interval $[0, T_l]$, where T_l – time corresponding to long-term creep. The time corresponding to short-term creep $T_s = 0.1T_c$ will also be used in the algorithm for determining the viscoelastic constants of the thermoset.

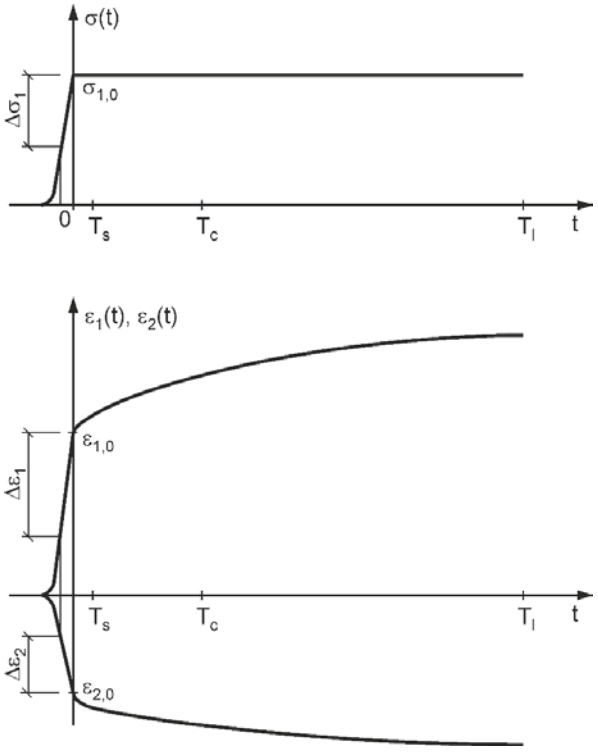

Fig. 7. General diagram of stress-controlled unidirectional tension creep test on thermoset

Determination of viscoelastic constants of thermoset

Viscoelastic constants c, r are dimensionless, while retardation time T_c is measured in minutes. The experimental tension creep test records directional strains $\varepsilon_1(t), \varepsilon_2(t)$. The time courses of the experimental shear and bulk strains are calculated from the well-known equations

$$\varepsilon_{s1e}(t) = \tfrac{2}{3}[\varepsilon_1(t) - \varepsilon_2(t)]\ ,\ \ \varepsilon_{be}(t) = \tfrac{1}{3}[\varepsilon_1(t) + 2\varepsilon_2(t)] \tag{43}$$

The control conditions are of the form

$$\varepsilon_{s1e}(0) = S_s\sigma_{s1e}\ ,\ \ \varepsilon_{be}(0) = S_b\sigma_{be} \tag{44}$$

where

$$\sigma_{s1e} = \tfrac{2}{3}\sigma_{1,0}\ ,\ \ \sigma_{be} = \tfrac{1}{3}\sigma_{1,0} \tag{45}$$

If the H-R/H rheological model is adequate for thermosets, then

$$\varepsilon_{s1e}(t) = [1 + c\varphi(\tau)]\varepsilon_{s1e}(0)\ ,\ \ \varepsilon_{be}(t) = \varepsilon_{be}(0)\ ,\ \ t \geq 0 \tag{46}$$

with $\tau = t/T_c$. In the identification algorithm, we will use the values of the simulation creep function corresponding to times $T_c,\ 0.1T_c$, i.e.

$$a = \varphi(1)\,,\ \ b = \varphi(0.1) \tag{47}$$

The readings from experimental graph $\varepsilon_{\mathrm{s1e}}(t)$ and the calculation accuracy will be given to 3 meaningful digits.

The analytical algorithm for identifying the viscoelastic constants of the thermoset, T_{c}, c, r, is based on Eqn. $(46)_1$ and is as follows:

1) prediction of the value of constant r based on a comparison of the gradients of experimental function $\varepsilon_{\mathrm{s1e}}(t)$ with the gradients of simulation creep function $\varphi(\tau)$, both functions on a semi-logarithmic scale;
2) prediction of the value of parameter $a(r)$;
3) reading abscissa $y = \log T_{\mathrm{c}}$ corresponding to the inflection point of graph $\varepsilon_{\mathrm{s1e}}(t)$ on a logarithmic time scale;
4) calculations:

$$T_{\mathrm{c}} = 10^{y} = \exp(y \ln 10)\,,\quad 0.1T_{\mathrm{c}}\,;$$

5) readings:

$$\varepsilon_{\mathrm{s1e}}(0), \varepsilon_{\mathrm{s1e}}(T_{\mathrm{c}}), \varepsilon_{\mathrm{s1e}}(0.1T_{\mathrm{c}})\,;$$

6) $\varepsilon_{\mathrm{s1e}}(T_{\mathrm{c}}) = (1 + c \cdot a)\varepsilon_{\mathrm{s1e}}(0) \implies$
$c = [\varepsilon_{\mathrm{s1e}}(T_{\mathrm{c}})/\varepsilon_{\mathrm{s1e}}(0) - 1]/a\,;$ (48)

7) $\varepsilon_{\mathrm{s1e}}(0.1T_{\mathrm{c}}) = (1 + c \cdot b)\varepsilon_{\mathrm{s1e}}(0) \implies$
$b = [\varepsilon_{\mathrm{s1e}}(0.1T_{\mathrm{c}})/\varepsilon_{\mathrm{s1e}}(0) - 1]/c\,;$ (49)

8) calculation of constant $r(b)$;
9) calculation of constant $a(b)$, comparison with the predicted value and iteration if necessary (return to point 6).

Once constants T_{c}, c, r are determined, the simulation shear strain vs. time can be calculated

$$\varepsilon_{\mathrm{s1}}(t) = [1 + c\varphi(\tau)]\varepsilon_{\mathrm{s1}}(0)\,,\ \varepsilon_{\mathrm{s1}}(t) = \varepsilon_{\mathrm{s1e}}(0)\,,\ \ t \in [0, T_{\mathrm{l}}] \tag{50}$$

and presented on a logarithmic time scale ($y = \log t$) against the experimental graph. In the registration interval of the creep process, we select a set of N quasi-equally spaced collocation points on a logarithmic time scale. From graph $\varepsilon_{\mathrm{s1e}}(t)$, experimental values $\varepsilon_{\mathrm{s1e}}(t_i)$, $t_i = 10^{y_i},\ \ i = 1, 2, \ldots, N$, are read. The relative error of the deviation of graph $\varepsilon_{\mathrm{s1}}(t)$ from graph $\varepsilon_{\mathrm{s1e}}(t)$ on a logarithmic time scale is

$$\delta = \textstyle\sum_{i=1}^{N} |\varepsilon_{\mathrm{s1}}(t_i) - \varepsilon_{\mathrm{s1e}}(t_i)| / \sum_{i=1}^{N} \varepsilon_{\mathrm{s1e}}(t_i) \tag{51}$$

whereby

$$\begin{gathered} \varepsilon_{\mathrm{s1}}(t_i) = [1 + c\varphi(\tau_i)]\varepsilon_{\mathrm{s1}}(0) \\ \tau_i = t_i/T_{\mathrm{c}},\ \ \varphi(\tau_i) = 1 - \textstyle\int_0^{\infty} \exp(-u\tau_i)\, L(u)\, du \end{gathered} \tag{52}$$

Constant r is contained in function $L(u)$.

Determination of effective elastic and viscoelastic constants of UFRT composite

According to the formulated elastic-viscoelastic model, composite UFRT is described by 5 viscoelastic constants, i.e. $c_1, c_4, c_5, r, T_{\mathrm{c}}$, where constants r, T_{c} also describe the thermoset matrix. Long-term creep coefficients c_1, c_4, c_5 will be determined using the viscoelastic-elastic correspondence principle (VECP).

Unconjugated standard constitutive equations of the linear elasticity of a homogenized UFRT composite (Eqns. A15-A.17) are expressed in terms of three quasi-shear/shear elastic compliances, i.e. $S_{\mathrm{s1}}, S_{\mathrm{s4}}, S_{\mathrm{s5}}$ (determined by Eqns. $(A.17)_{3,4}$, $(A.14)_8$). From Eqns. $(A.17)_3$, $(A.14)_{3,5}$, we obtain the first compliance corresponding to the homogenized composite, i.e.

$$S_{\mathrm{s1,h}} = S_{11,\mathrm{h}} - \lambda S_{12,\mathrm{h}} \tag{53}$$

As a result of the homogenization of composite UFRT, the elastic compliances $S_{\mathrm{s}j,\mathrm{h}}(s_{\mathrm{s}}, s_{\mathrm{b}}),\ \ j = 1, 4, 5$, are dependent on dimensionless elastic compliances $s_{\mathrm{s}}, s_{\mathrm{b}}$ of the polymeric matrix defined in Eqns. $(5)_{3,4}$.

As a result of the homogenization of a UFRT composite, elastic compliances $S_{\mathrm{s}j,\mathrm{h}}(s_{\mathrm{s}}, s_{\mathrm{b}}),\ j = 1, 4, 5$, depend on dimensionless elastic compliances of the polymeric matrix, $s_{\mathrm{s}}, s_{\mathrm{b}}$, defined in Eqns. $(5)_{3,4}$.

The complex compliances of the UFRT composite, corresponding to the H-R/H rheological model, result from Eqns. $(A.18)_1$, (A.22). They can be written in the following dimensionless form:

$$\begin{gathered} s^{*}_{\mathrm{s}j}(\alpha) = s'_{\mathrm{s}j}(\alpha) + \mathrm{i}s''_{\mathrm{s}j}(\alpha)\,,\ \ s^{*}_{\mathrm{s}j}(\alpha) = S^{*}_{\mathrm{s}j}(\alpha)/S_{\mathrm{s}j}\,, \alpha = \omega T_{\mathrm{c}}\,,\ \ j = 1, 4, 5 \\ s'_{\mathrm{s}j}(\alpha) = 1 + c_j M'(\alpha)\,,\ \ s''_{\mathrm{s}j}(\alpha) = -c_j M''(\alpha) \\ M'(\alpha) = \frac{1 + \alpha^r \cos(\pi r/2)}{1 + 2\alpha^r \cos(\pi r/2) + \alpha^{2r}}\,, M''(\alpha) = \frac{\alpha^r \sin(\pi r/2)}{1 + 2\alpha^r \cos(\pi r/2) + \alpha^{2r}} \end{gathered} \tag{54}$$

The complex compliances of a UFRT composite can also be determined using the VECP, i.e.

$$\begin{gathered} s^{*}_{\mathrm{s}j,\mathrm{h}}(\alpha) = s'_{\mathrm{s}j,\mathrm{h}}(\alpha) + \mathrm{i}s''_{\mathrm{s}j,\mathrm{h}}(\alpha) = S_{\mathrm{s}j,\mathrm{h}}[s^{*}_{\mathrm{s}}(\alpha), s_{\mathrm{b}}]/S_{\mathrm{s}j}\ ,\ \ j = 1, 4, 5 \\ s^{*}_{\mathrm{s}}(\alpha) = s'_{\mathrm{s}}(\alpha) + \mathrm{i}s''_{\mathrm{s}}(\alpha)\,,\ \ s'_{\mathrm{s}}(\alpha) = s_{\mathrm{s}}[1 + cM'(\alpha)]\,, \\ s''_{\mathrm{s}}(\alpha) = -s_{\mathrm{s}} c M''(\alpha) \end{gathered} \tag{55}$$

Variable α is defined in Eqn. $(54)_3$.

Viscoelastic constants c_1, c_4, c_5 are determined from the following conditions:

$$s'_{\mathrm{s}j}(\alpha_d) = s'_{\mathrm{s}j,\mathrm{h}}(\alpha_d)\,,\ \ j = 1, 4, 5 \tag{56}$$

where α_d is the value of α for which conditions $M'(\alpha) \approx \approx 0.5,\ \ M''(\alpha) = \min$ are met. After inserting Eqn. $(54)_4$ into Eqn. (56), we obtain

$$c_j = \left[s'_{\mathrm{s}j,\mathrm{h}}(\alpha_d) - 1\right]/M'(\alpha_d)\ ,\ \ j = 1, 4, 5 \tag{57}$$

The loss compliances have small values compared to the storage compliances, i.e. they are less conditioned.

The relative error of deviation of graphs $s'_{\mathrm{s}j}(\alpha), s'_{\mathrm{s}j,\mathrm{h}}(\alpha), j = 1, 4, 5$, is

$$\delta = \textstyle\sum_{i=1}^{n} |s'_{\mathrm{s}j}(\alpha_i) - s'_{\mathrm{s}j,\mathrm{h}}(\alpha_i)| / \sum_{i=1}^{n} s'_{\mathrm{s}j,\mathrm{h}}(\alpha_i) \tag{58}$$

whereby $\alpha_i = 2\pi y_i,\ \ y_i = i \cdot \Delta y,\ \ i = 1, 2, \ldots, n.$

EXPERIMENTAL TEST AND NUMERICAL TESTS

Experimental test

The experimental creep test was performed on a new sample made of 'Polimal 109' structural unsaturated polyester resin (former manufacturer: 'Organika Sarzyna' Chemical Plants, Sarzyna, Poland). The test was performed in 2002 at normal conditions, using a lever creeper.

According to the Technical Data Sheet of the 'Polimal 109' resin, the basic material constants of this resin are: tensile strength $R_\mathrm{t} = 70$ MPa, Young's modulus for tension $E = 4.30$ GPa, ultimate longitudinal strain $\varepsilon_\mathrm{t} = 2\% = 0.02 = 20000$ μs, heat distortion temperature $T_\mathrm{h} = 63$°C, where μs denotes micro strain (1 μs $= 10^{-6}$).

The tension creep test was performed according to the experiment description. In Phase 2, the normal longitudinal stress was $\sigma_{1,0} = 0.15R_\mathrm{t} = 10.5$ MPa, which guaranteed reversibility of the creep process. On the basis of Phase 1 (elastic) of the loading process for this specimen, the following parameters were identified (technical accuracy of 3 meaningful digits):

$$E = 4.28\ \mathrm{GPa}\,,\quad \nu = 0.363$$
$$\varepsilon_1(0) = 2450\ \mu\mathrm{s}\,,\quad \varepsilon_2(0) = -892\ \mu\mathrm{s}$$
$$\varepsilon_{\mathrm{s1e}} = 2230\ \mu\mathrm{s}\,,\quad \varepsilon_{\mathrm{be}} = 223\ \mu\mathrm{s}$$

Figure 8 shows graphs of the directional strains vs. time in the reversible creep test with unidirectional tension, recorded in interval $[0, T_\mathrm{l}]$, $T_\mathrm{l} = 10^5$ min. Progressive recording intervals from 0.005 min at the beginning of the process to 275 min at the end of the process were used. Figures 9 and 10 (zoom) show the time courses of the directional strain rates calculated approximately according to the formula

$$\dot{\varepsilon}_j(t_i) = d\varepsilon_j/dt \approx \left[\varepsilon_j(t_{i+10}) - \varepsilon_j(t_i)\right]/(t_{i+10} - t_i),$$
$$j = 1, 2,\quad i = 1, 2, \ldots \tag{59}$$

According to the theoretical prediction of reversible creep, the strain rates decrease in Phase 2. Very large values of the strain rates were observed at the beginning of the time interval, which decreased to very small values for $t > 10^4$ min i.e.

$$\dot{\varepsilon}_1(0.1) = 132\ \mu\mathrm{s/min}\,,\quad \dot{\varepsilon}_2(0.1) = -57\ \mu\mathrm{s/min}$$
$$\dot{\varepsilon}_1(80000) = 0.010\ \mu\mathrm{s/min}\,,\quad \dot{\varepsilon}_2(80000) = -0.005\ \mu\mathrm{s/min}$$

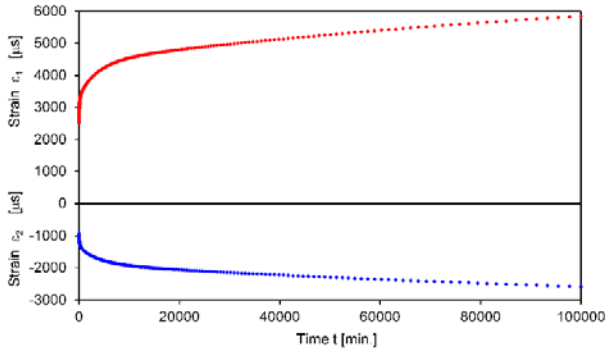

Fig. 8. 'Polimal 109' polyester resin thermoset. Directional strains in experimental creep test with unidirectional tension

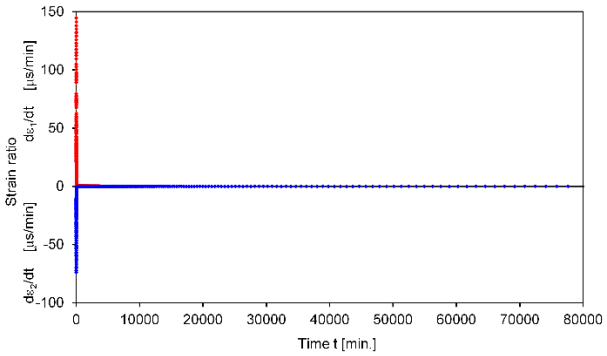

Fig. 9. 'Polimal 109' polyester resin thermoset. Directional strain rates in experimental creep test with unidirectional tension

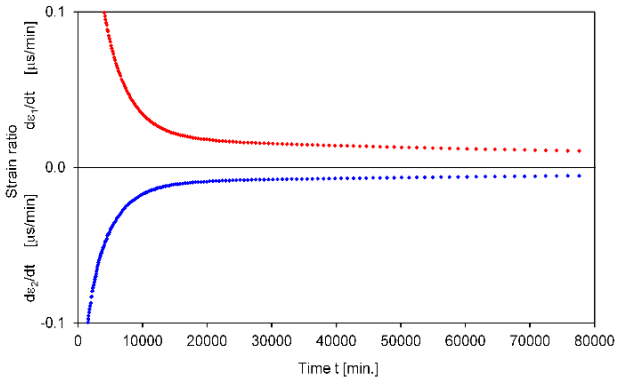

Fig. 10. 'Polimal 109' polyester resin thermoset. Directional strain rates in experimental creep test with unidirectional tension (zoom)

Figure 11 shows the directional strains of the sample in the experimental creep test with unidirectional tension, on a logarithmic time scale.

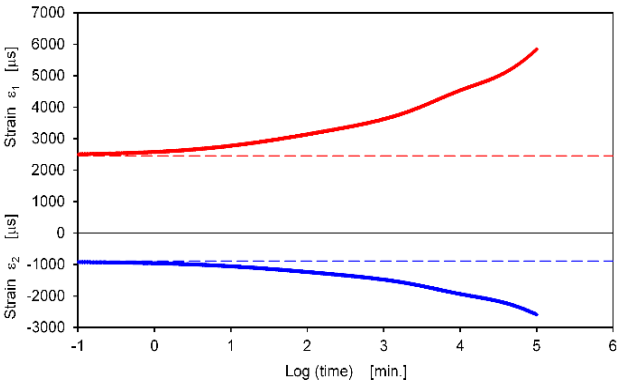

Fig. 11. 'Polimal 109' polyester resin thermoset. Directional strains in experimental creep test with unidirectional tension, on logarithmic time scale

The levels of the initial (elastic) deformation are indicated by dashed lines. As expected, a long-term creep time, $T_\mathrm{l} = 10^5$ min. (~70 days), would have to be extended at least 10 times to prove the creep reversibility hypothesis. Moreover, the reverse creep test (recovery test) would be required. The interpretation of small oscillations in the directional strain patterns on a logarithmic time scale requires additional creep tests on a set

of samples, with monitoring of the temperature, humidity and material aging.

Figure 12 shows the shear and bulk strains of the sample in the experimental creep test with unidirectional tension, on a logarithmic time scale. The levels of the initial (elastic) deformation are marked with dashed lines. Transformation of the directional strains was performed according to Eqns. (43). The constant bulk strain hypothesis was confirmed.

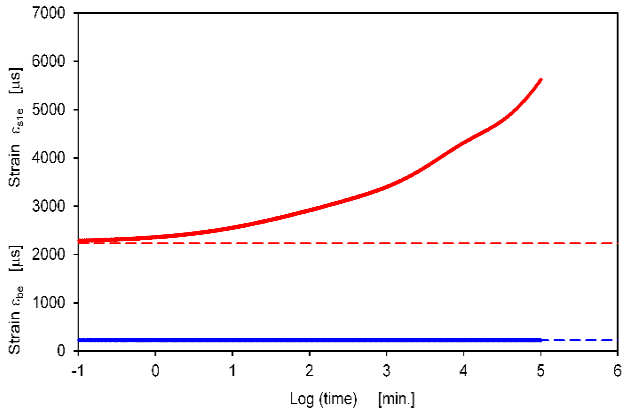

Fig. 12. 'Polimal 109' polyester resin thermoset. Shear and bulk strains in experimental creep test with unidirectional tension, on logarithmic time scale

Software

Numerical calculations were performed using an original programme written in the Pascal language. The computational algorithms are described in Section 3. The programme has 7 computational paths:

1) Testing the accuracy of the integration of improper integrals with a fractional exponential generic function, by means of Gauss-Legendre quadratures.
2) Analysis of a creep function described by a fractional exponential generic function.
3) Analysis of the complex compliance of a thermoset, corresponding to a fractional exponential generic function.
4) Identification of the viscoelastic constants of an exemplary thermoset, corresponding to the H-R/H rheological model.
5) Determination of the elastic constants of an exemplary UFRT composite, according to the modified homogenization theory.
6) Analysis of the complex compliances of a UFRT composite, corresponding to a fractional exponential generic function.
7) Identification of the viscoelastic constants of an exemplary UFRT composite, corresponding to the H-R/H rheological model.

The accuracies adopted are as follows: accuracy of input data: 3 meaningful digits; calculation accuracy: double precision; result accuracy: 3 meaningful digits. The results were output as text files and transferred to Excel sheets to create the final graphs.

Gauss-Legendre quadrature testing

Testing the accuracy of the integration of improper integrals using Gauss-Legendre quadratures, with a subintegral function containing a fractional exponential generic function, was performed for integral $J = \int_0^\infty L(u)\,du = 1$, according to Eqn. (41). Quadratures of degrees $n = 15, 25, 32$ were applied; the nodes and weights were taken from Ref. [12]. The integration was performed for $r \in [0.30, 0.98]$.

Figure 13 presents the graphs of the relative error $\delta = |1 - J| \cdot 100\%$. In further calculations the most accurate quadrature of degree available $n = 32$ was used; in subinterval $r \in [0.55, 0.95]$ error $\delta < 1\%$, and in subinterval r ∈ [0.36,0.54] error $\delta \in [1\%, 7\%]$. The given errors are technically acceptable, but for fraction r of the order 0.40 a quadrature of a much higher degree is desirable.

Creep function analysis

The graphs of creep function $\varphi(\tau)$, $\tau = t/T_c$, were computed according to Eqn. (41). The simulations were performed in interval $\tau \in [10^{-2}, 10^4]$, for $r = 0.33,\ 0.40, 0.50, 0.60, 1$. The graph corresponding to the H-K/H model ($r = 1$) is the reference graph. In order to reveal the features of the H-R/H rheological model, the creep function graphs are shown on a semi-logarithmic scale with x as the abscissa, with

$$x = \log\tau = \ln\tau/\ln 10\,,\ \tau = 10^x = \exp(x \ln 10)\ ,\ x \in [-2,\ 4] \tag{60}$$

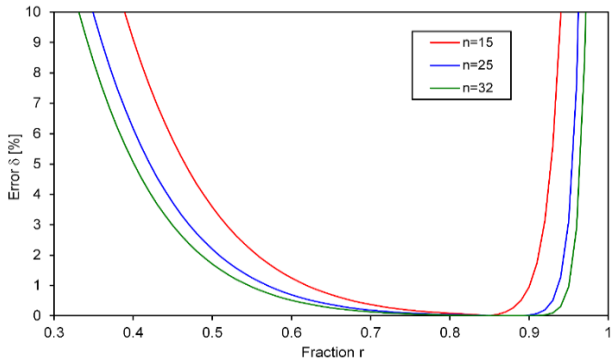

Fig. 13. Integration error $\boldsymbol{\delta(r)}$ [%]

The graphs of the creep function for the mentioned values of r are shown in Figure 14. Function $\varphi(\tau)$ on a semi-logarithmic scale is increasing, containing one inflection point. The slope of the graph at the inflection point decreases with decreasing fraction r.

Time point $t = T_c$ corresponds to $\tau = 1$, $x = 0$. Time point $t = 0.1T_c$ corresponds to $\tau = 0.1$, $x = -1$. The values of the creep function at characteristic points $T_c, 0.1T_c$, used in the algorithm for identification of the viscoelastic constants of a thermoset, are summarized in Table 2. Function $a(r)$ has a quasi-constant course, while function $b(r)$ is quasi-linear.

TABLE 2. **Values of creep function $\varphi(\tau)$ at characteristic points**

	r				
	0.33	**0.40**	**0.50**	**0.60**	**1**
$a=\varphi(1)$	0.598	0.583	0.581	0.589	0.632
$b=\varphi(0.1)$	0.405	0.347	0.285	0.235	0.095

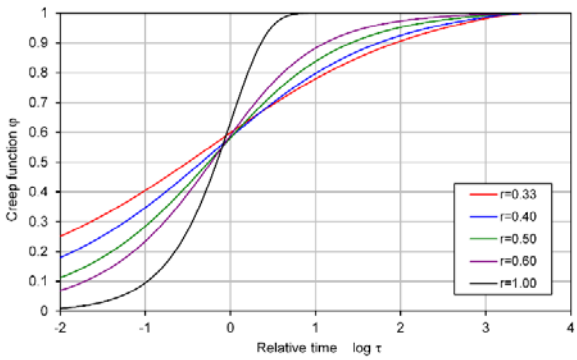

Fig. 14. Graphs of creep function $\boldsymbol{\varphi(\tau)}$ on semi-logarithmic scale, corresponding to selected values of $\boldsymbol{r}$

Analysis of complex compliance of thermoset

The complex compliance of a thermoset is described by Eqns. (23), $(3)_8$ presented in Ref. [1]. At this stage of the numerical tests it is not necessary to introduce modulus E_f. The relative complex compliance of a thermoset is described by the following formulae:

$$S_\mathrm{s}^*(\alpha)=S_\mathrm{s}'(\alpha)+\mathrm{i}S_\mathrm{s}''(\alpha)\,,\quad S_\mathrm{s}'(\alpha)=S_\mathrm{s}[1+cM'(\alpha)]\,,$$
$$S_\mathrm{s}''(\alpha)=-S_\mathrm{s}cM''(\alpha)$$
$$S_\mathrm{s}=1/2G\,,\qquad s_\mathrm{s}^*(\alpha)=s_\mathrm{s}'(\alpha)+\mathrm{i}s_\mathrm{s}''(\alpha)\,,$$
$$\alpha=\omega T_\mathrm{c}=2\pi x,\quad x\in[0,\ 4]$$
$$s_\mathrm{s}'(\alpha)=S_\mathrm{s}'(\alpha)/S_\mathrm{s}=1+cM'(\alpha)\,,$$
$$s_\mathrm{s}''(\alpha)=S_\mathrm{s}''(\alpha)/S_\mathrm{s}=-cM''(\alpha) \qquad (61)$$

whereby functions $M'(\alpha), M''(\alpha)$, depending on viscoelastic constant r, are defined by Eqns. $(54)_{6,7}$. The adopted range of values of dimensionless variable x is sufficient for analysis of the characteristics of the relative storage and loss compliances $s_\mathrm{s}'(\alpha), s_\mathrm{s}''(\alpha)$. Step $\Delta x=0.01$ was adopted. The complex compliance analysis of a thermoset was carried out for constant $c=2$ as an example.

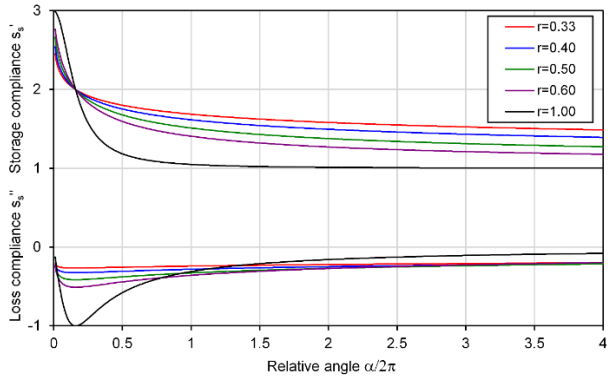

Fig. 15. Relative storage and loss compliances vs. variable $\boldsymbol{x}$, corresponding to selected values of $\boldsymbol{r}$

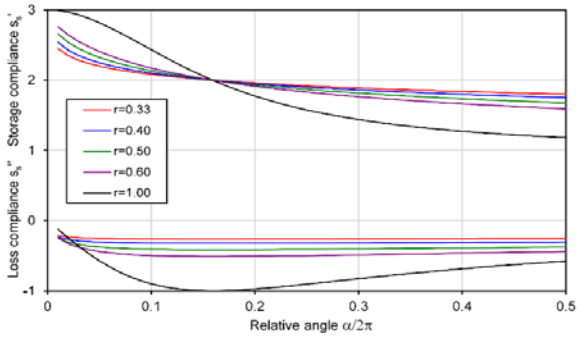

Fig. 16. Relative storage and loss compliances vs. variable $\boldsymbol{x}$, corresponding to selected values of $\boldsymbol{r}$ (zoom)

Figures 15 and 16 show the relative storage and loss compliances vs. variable x, for selected values of constant r. The reference graphs correspond to $r=1$. At $x=0.159$ a node of curves $s_\mathrm{s}'(\alpha)$ is formed. At this point $s_\mathrm{s}'(\alpha)\approx 1+c/2,\ \ s_\mathrm{s}''(\alpha)=\min$. This point was used in the algorithm to identify the viscoelastic constants of the UFRT composite, i.e. $\alpha=2\pi\cdot 0.159=$ $=0.318\pi$. The gradient of $s_\mathrm{s}'(\alpha)$ at the nodal point decreases with a decreasing value of r.

Identification of viscoelastic constants of 'Polimal 109' thermoset

An algorithm for identifying the viscoelastic constants of a thermoset was formulated in in this study. The identification was performed for the 'Polimal 109' resin. The identification calculations in the final iteration are as follows:

1) predicted value: $r=0.37$;
2) reading from Table 2: $a(r)=0.59$;
3) reading abscissa corresponding to the point of inflection of graph $\varepsilon_{\mathrm{s1e}}(t)$ on a semi-logarithmic scale, without taking into account the disturbing oscillations: $y=4.84$;
4) $T_\mathrm{c}=\exp(4.84\ln 10)=69200$ min, $0.1T_\mathrm{c}=$ 6920 min;
5) readings: $\varepsilon_{\mathrm{s1e}}(0)=2230$ μs, $\varepsilon_{\mathrm{s1e}}(T_\mathrm{c})=5280$ μs, $\varepsilon_{\mathrm{s1e}}(0.1T_\mathrm{c})=4160$ μs;
6) $c=[5280/2230-1]/0.59=2.32$;
7) $b=[4160/2230-1]/2.32=0.373$;
8) $r(b)=0.370$;
9) $a(b)=0.590$.

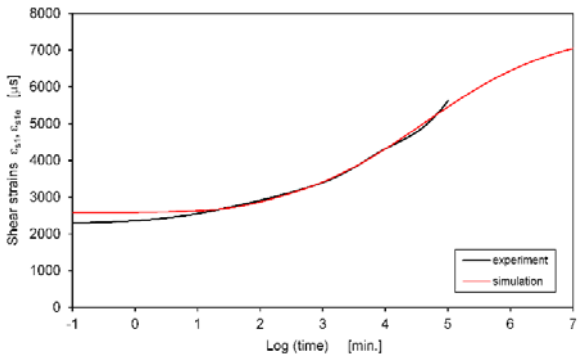

Fig. 17. Simulated shear strain graph $\boldsymbol{\varepsilon_{s1}(t)}$ against experimental shear strain graph $\boldsymbol{\varepsilon_{s1e}(t)}$

The results of the identification of the viscoelastic constants of the 'Polimal 109' resin are therefore as follows: $T_c = 69200$ min., $c = 2.32$, $r = 0.370$. The relative error of the deviation of the $\varepsilon_{s1}(t)$ curve from the $\varepsilon_{s1e}(t)$ curve on a logarithmic time scale, calculated in interval $y \in [-1, 5]$, is $\delta = 3.1\%$ (Fig. 17). In interval $y \in [-1, 0.90]$, i.e. for small values of time $t \in [0.1 \text{ min.}, 8 \text{ min.}]$, the H-R/H model slightly overestimates the shear strains. In the technically relevant interval $y \in [1, 5]$, i.e. $t \in [10 \text{ min.}, 100000 \text{ min}]$, the H-R/H model is fully adequate (100000 min ≈ ≈ 70 days). The long-term shear strain value predicted by Eqn. $(46)_1$ is $\varepsilon_{s1e}(\infty) = (1 + c \cdot 1) \cdot \varepsilon_{s1e}(0) = 7400$ μs. The long-term relaxation coefficient and relaxation time of the 'Polimal 109' resin (calculated from Eqns. $(25)_3$, (29) given in Ref. [1]) are: $d = 0.70$, $T_d = 2700$ min.

Determination of elastic constants of UFRT composite

The assumptions for a UFRT composite are summarized in Introduction. The modified homogenization theory of a UFRT composite is presented in second Section. The elastic constants of a UFRT composite are calculated analytically from Eqns. (37).

A UFRT composite made of the following components was chosen as the illustrative material:

- matrix: unsaturated polyester resin 'Polimal 109' (linearly viscoelastic isotropic material) with elastic constants $E = 4.28$ GPa, $\nu = 0.363$;
- reinforcing fibres: E-glass (linearly elastic isotropic material) with elastic constants $E_f = 72.4$ GPa, $\nu = 0.220$;
- fibre volume fraction $f = 0.50$ (vacuum infusion technology).

The predicted values of the independent elastic constants of the homogenized UFRT composite (linearly elastic monotropic material) are:

$$E_1 = 38.4 \text{ GPa}, \quad E_2 = 9.72 \text{ GPa}, \quad \nu_{21} = 0.285,$$
$$\nu_{32} = 0.526, \quad G_{12} = 4.14 \text{ GPa}$$

In addition, $G_{23} = 3.18$ GPa, $\nu_{12} = 0.0721$, $\lambda = 0.137$.

Determination of complex compliances and viscoelastic constants of UFRT composite

Viscoelastic constants c_1, c_4, c_5 of the tested UFRT composite, calculated analytically with a technical accuracy of 0.01 from Eqns. (57), are:

$$c_1 = 0.07, \quad c_4 = 2.18, c_5 = 2.04.$$

H-R/H storage compliance graphs $s'_{sj}(\alpha)$ against VECP storage compliance graphs $s'_{sj,h}(\alpha)$ are presented in Figures 18-20 for $j = 1, 4, 5$ respectively.

The long-term relaxation coefficients and relaxation times of the tested UFRT composite (calculated from Eqns. $(A.24)_{5,6}$) are:

$$d_1 = 0.065, \quad d_4 = 0.69, \quad d_5 = 0.67, T_{d_5} = 3430 \text{ min}$$
$$T_{d_1} = 57600 \text{ min}, \quad T_{d_4} = 3040 \text{ min},$$

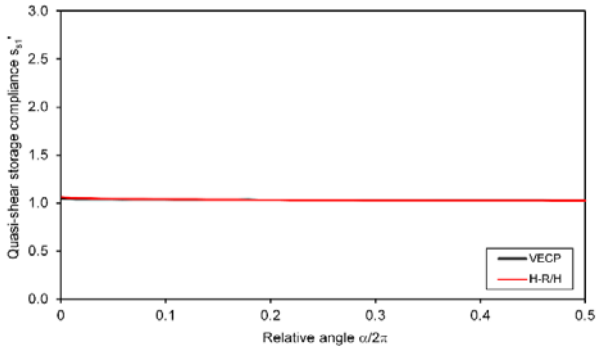

Fig. 18. H-R/H storage compliance $s'_{s1}(\alpha)$ against VECP storage compliance $s'_{s1,h}(\alpha)$

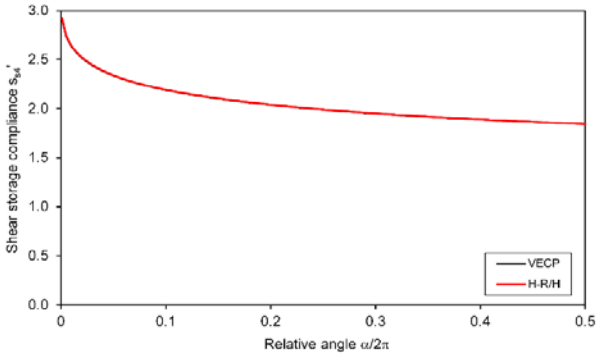

Fig. 19. H-R/H storage compliance $s'_{s4}(\alpha)$ against VECP storage compliance $s'_{s4,h}(\alpha)$

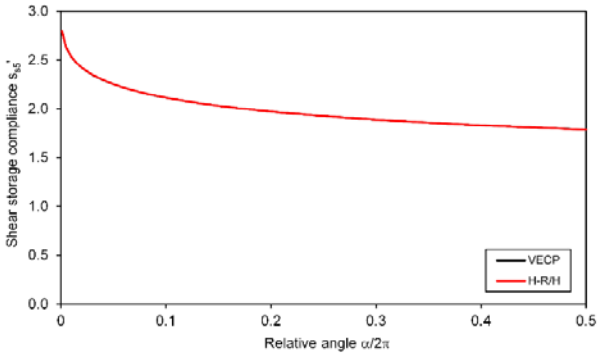

Fig. 20. H-R/H storage compliance $s'_{s5}(\alpha)$ against VECP storage compliance $s'_{s5,h}(\alpha)$

The conclusions resulting from analysis of the graphs shown in Figures 18-20 are as follows:

- The relative deviation errors of the H-R/H and VECP curves, calculated in interval $y \in [0, 0.5]$, are $\delta = 0.3\%, 0.05\%, 0.005\%$ for $s'_{s1}, s'_{s4}, s'_{s5}$, respectively. The H-R/H rheological model of UFRT composites formulated in Ref. [1] is fully confirmed.
- The hypothesis that the rheological properties of UFRT composites are described by viscoelastic constants r, T_c of the thermoset matrix was also fully confirmed.

- The shear creep in the monotropy and transverse isotropy planes of UFRT composites, described by viscoelastic constants c_4, c_5, is dominant. The reinforcing fibres slightly reduce long-term creep coefficients c_4, c_5 compared to long-term creep coefficient c of the pure thermoset.
- Long-term creep coefficient c_1 is approximately 3.5% of creep factor c_4 or c_5. The elastic fibres are very effective at suppressing the viscoelasticity of URFT composites under tension/compression in the fibre direction.

CONCLUSIONS

The study constituted Part 2 of advanced analytical modelling of the linear elasticity and viscoelasticity of thermosets and unidirectional long glass fibre-reinforced thermoset-matrix (UFRT) composites. New rheological models (coded H-R/H) for thermosets and UFRT composites, described by the smallest possible number of the material constants, were tested by experiment and simulation. The generic function for viscoelastic shear/quasi-shear stresses in thermosets and UFRT composites was assumed as the Mittag-Leffler fractional exponential function in an integral form. The key modelling tools relative to UFRT composites were: the modified homogenization theory and VECP.

The modified homogenization theory for UFRT composites, based on the selected tasks of the linear theory of elasticity, was positively validated on the exemplary E-glass fibre/vinyl-ester resin composite. The 32-point Gauss-Legendre quadrature proved necessary to calculate improper integrals involving a fractional exponential generic function.

The elastic (E, ν) and viscoelastic (r, T_c, c) constants of the exemplary thermoset ('Polimal 109' unsaturated polyester resin) that describe the H-R/H rheological model in normal conditions were determined with technical accuracy, based on the experimental unidirectional tension creep test. The elastic $(E_1, E_2, \nu_{21}, \nu_{32}, G_{12})$ and viscoelastic (r, T_c, c_1, c_4, c_5) constants of the exemplary UFRT composite ('Polimal 109' unsaturated polyester resin matrix reinforced with long E-glass fibres) that describe the H-R/H model in normal conditions were determined with technical accuracy.

Based on the exemplary materials, the following final conclusions can be formulated:

1. The H-R/H rheological model is adequate for thermosets in technically relevant interval $t \in [10\ \text{min}, 100000\ \text{min}]$. The shear deformations are viscoelastic but the bulk deformations are elastic.
2. The H-R/H rheological model is adequate for UFRT composites in technically relevant interval $t \in [10\ \text{min}, 100000\ \text{min}]$. The quasi-shear and shear deformations are viscoelastic but the quasi-bulk deformations are elastic.
3. Two viscoelastic constants, i.e. fraction r of the viscoelasticity generic function, and retardation time T_c, are common to the thermoset matrix and the UFRT composite.
4. Shear creep in the monotropy and transverse isotropy planes of UFRT composites is dominant. The elastic fibres are very effective at suppressing the viscoelasticity of URFT composites under tension/compression in the fibre direction.

The presented series of publications also offers research teams developing the rheology of thermosets and thermoset-matrix composites reinforced with stitched glass fabrics possible cooperation in the following fields:

- modified procedures for experimental determining the elastic constants of thermosets and UFRT composites;
- long-term unidirectional tension creep/recovery experimental tests on selected thermosets, for selected stress and temperature levels, with a minimum of 5 specimens in each case;
- determination of the elastic and viscoelastic constants for selected thermosets, based on relevant experimental tests;
- experimental validation of the elastic constants predicted by the modified homogenization theory for selected UFRT composites;
- testing Gauss-Legendre quadratures of very high order ($n \gg 32$);
- experimental validation of the H-R/K rheological model for selected thermosets;
- experimental validation of the H-R/K rheological model for selected UFRT composites;
- implementation of the H-R/K model into a selected CAE system;
- experimental validation of the H-R/K rheological model for selected stitched glass fabric-reinforced thermoset-matrix laminates.

Acknowledgements

The identification tests described in Section 2 were conducted in 2014 at the Materials and Structures Research Laboratory, Faculty of Mechanical Engineering, Military University of Technology, Warsaw, Poland, as a part of research project No. PBS1/B2/6/2013, which received funding from the National Centre for Research and Development, Poland. The creep test described in Section 4 was conducted in 2002 at the same institution, as a part of research project No. 7 T08E 011 18, which received funding from the Scientific Research Committee, Poland. Proofreading of the manuscript was done by Mrs. Christine Frank-Szarecka, Canada. These supports are gratefully acknowledged.

APPENDIX A. SELECTED FINAL FORMULAS FROM REF. [1]

Shear and bulk modules of a thermoset are defined as

$$G = E/2(1+\nu),\ B = E/3(1-2\nu) \qquad \text{(A.1)}$$

where: E, ν – elastic constants (Young's modulus, Poisson's ratio).

Conjugated standard constitutive equations of the linear elasticity of a thermoset, written in matrix notation, have the form:

$$\boldsymbol{\varepsilon} = \mathbf{S}\,\boldsymbol{\sigma}\,, \quad \boldsymbol{\delta} = S_{\mathrm{s}}\,\boldsymbol{\tau} \tag{A.2}$$

where

$$\boldsymbol{\varepsilon} = \begin{bmatrix}\varepsilon_1\\ \varepsilon_2\\ \varepsilon_3\end{bmatrix},\ \boldsymbol{\delta} = \begin{bmatrix}\delta_{23}\\ \delta_{13}\\ \delta_{12}\end{bmatrix},\ \boldsymbol{\sigma} = \begin{bmatrix}\sigma_1\\ \sigma_2\\ \sigma_3\end{bmatrix},\ \boldsymbol{\tau} = \begin{bmatrix}\tau_{23}\\ \tau_{13}\\ \tau_{12}\end{bmatrix}$$
$$\mathbf{S} = \begin{bmatrix}S_{11} & S_{12} & S_{12}\\ S_{12} & S_{11} & S_{12}\\ S_{12} & S_{12} & S_{11}\end{bmatrix},\ S_{11} = 1/E\,,\ S_{12} = -\nu/E\,,\ S_{\mathrm{s}} = 1/2G \tag{A.3}$$

with $\delta_{jk} = \gamma_{jk}/2\,, jk = 23, 13, 12$ (γ_{jk} – shear strains). Vectors $\boldsymbol{\varepsilon}, \boldsymbol{\delta}, \boldsymbol{\sigma}, \boldsymbol{\tau}$ represent parts of the strain and stress tensors at point (x_1, x_2, x_3), respectively. Matrix $\mathbf{S}$ is the elastic compliance matrix and coefficient S_{s} is the elastic shear compliance of a thermoset. Equations $(A.2)_2$ are unconjugated. The x_1, x_2, x_3 Cartesian coordinate system is consistent with directions of monotropy (transverse isotropy) of a UFRT composite.

Unconjugated standard constitutive equations of the linear elasticity-viscoelasticity of a thermoset have the form:

$$\begin{gathered}\boldsymbol{\varepsilon}_{\mathrm{s}}(t) = \tilde{S}_{\mathrm{s}}(t) \otimes \boldsymbol{\sigma}_{\mathrm{s}}(t)\,,\quad \varepsilon_{\mathrm{b}}(t) = S_{\mathrm{b}}\,\sigma_{\mathrm{b}}(t)\\ \boldsymbol{\delta}(t) = \tilde{S}_{\mathrm{s}}(t) \otimes \boldsymbol{\tau}(t)\end{gathered} \tag{A.4}$$

for time variable $t \geq 0$, with

$$\tilde{S}_{\mathrm{s}}(t) = S_{\mathrm{s}}\left[1 + c\int_0^t \Phi(v)\,dv\right],\quad \Phi(t) = \frac{1}{T_{\mathrm{c}}}\int_0^\infty \exp\left(-\frac{ut}{T_{\mathrm{c}}}\right) u\,L(u)\,du$$
$$L(u) = \frac{\sin \pi r}{\pi u}\frac{u^r}{1+2u^r\cos\pi r + u^{2r}}\,,\quad 0 < r < 1,\ S_{\mathrm{b}} = 1/3B \tag{A.5}$$

The nomenclature and interpretation are as follows: $L(u)$ – function creating the fractional exponential function in an integral form, r – fraction creating the fractional exponential function, T_{c} – retardation time, $\Phi(t)$ – generic function for shear stresses (the Mittag-Leffler fractional exponential function in an integral form), $\tilde{S}_{\mathrm{s}}(t)$ – elastic-viscoelastic shear compliance, c – long-term creep coefficient, $\otimes$ – convolution product operator.

The creep function for a thermoset is described by the formula:

$$\varphi(t) = \int_0^t \Phi(v)\,dv = 1 - \int_0^\infty \exp\left(-\frac{ut}{T_{\mathrm{c}}}\right) L(u)\,du \tag{A.6}$$

Functions $L(u), \Phi(t), \varphi(t)$ have the following properties:

$$\begin{gathered}L(u) \geq 0 \ \text{ for } \ u \geq 0\,,\quad \int_0^\infty L(u)\,du = 1\,,\quad \lim_{u\to 0_+} L(u) = \infty\\ \Phi(t) > 0 \ \text{ for } \ t > 0\,,\quad \lim_{t\to 0_+}\Phi(t) = \infty\,,\quad \lim_{t\to\infty}\Phi(t) = 0\\ \varphi(0) = 0\,,\quad \varphi(\infty) = \lim_{t\to\infty}\varphi(t) = 1\end{gathered} \tag{A.7}$$

The elastic-viscoelastic steady-state response in strains for a thermoset corresponding to the harmonic stress programme is

$$\boldsymbol{\varepsilon}_{\mathrm{s}}^*(t) = S_{\mathrm{s}}\left[1 + c\int_0^\infty \exp(-\mathrm{i}\omega v)\,\Phi(v)\,dv\right]\boldsymbol{\sigma}_{\mathrm{s}}^*(t) = S_{\mathrm{s}}^*(\omega)\,\boldsymbol{\sigma}_{\mathrm{s}}^*(t) \tag{A.8}$$

where

$$\begin{gathered}S_{\mathrm{s}}^*(\omega) = S_{\mathrm{s}}\left[1 + c\,\overline{\Phi}(\mathrm{i}\omega)\right] = S_{\mathrm{s}}\left[1 + c\frac{1}{1+(\mathrm{i}\omega T_{\mathrm{c}})^r}\right] = S_{\mathrm{s}}'(\omega) + \mathrm{i}S_{\mathrm{s}}''(\omega)\\ S_{\mathrm{s}}'(\omega) = S_{\mathrm{s}}\left[1 + c\frac{1+(\omega T_{\mathrm{c}})^r\cos(\pi r/2)}{1+2(\omega T_{\mathrm{c}})^r\cos(\pi r/2)+(\omega T_{\mathrm{c}})^{2r}}\right]\\ S_{\mathrm{s}}''(\omega) = -S_{\mathrm{s}}c\frac{(\omega T_{\mathrm{c}})^r\sin(\pi r/2)}{1+2(\omega T_{\mathrm{c}})^r\cos(\pi r/2)+(\omega T_{\mathrm{c}})^{2r}}\end{gathered} \tag{A.9}$$

with the following interpretation and nomenclature: $S_{\mathrm{s}}^*(\omega)$ – complex shear compliance, $S_{\mathrm{s}}'(\omega)$ – shear storage compliance (real part of the complex shear compliance), $S_{\mathrm{s}}''(\omega)$ – shear loss compliance (imaginary part of the complex shear compliance), ω – circular frequency, i – imaginary unit.

A long-term relaxation coefficient and a relaxation time are expressed in terms of constants c, T_{c}, i.e.

$$d = \frac{c}{1+c},\quad T_{\mathrm{d}} = T_{\mathrm{c}}\exp\left(\frac{1}{r}\ln\frac{1}{1+c}\right) \tag{A.10}$$

Conjugated standard constitutive equations of the linear elasticity and viscoelasticity of a thermoset have the form

$$\boldsymbol{\varepsilon}(t) = \tilde{\mathbf{S}}(t) \otimes \boldsymbol{\sigma}(t)\,,\quad \boldsymbol{\delta}(t) = \tilde{S}_{\mathrm{s}}(t) \otimes \boldsymbol{\tau}(t) \tag{A.11}$$

where

$$\tilde{\mathbf{S}}(t) = \tilde{S}_{\mathrm{s}}(t)\,(\mathbf{I} - \mathbf{A}) + S_{\mathrm{b}}\,\mathbf{A} \tag{A.12}$$

is the elastic-viscoelastic compliance matrix of a homogeneous isotropic material.

Conjugated standard constitutive equations of the linear elasticity of a homogenized UFRT composite are written in the form

$$\boldsymbol{\varepsilon} = \mathbf{S}\boldsymbol{\sigma}\,,\quad \boldsymbol{\delta} = \{\mathbf{S}\}\boldsymbol{\tau} \tag{A.13}$$

where

$$\mathbf{S} = \begin{bmatrix}S_{11} & S_{12} & S_{12}\\ S_{12} & S_{22} & S_{23}\\ S_{12} & S_{23} & S_{22}\end{bmatrix},\quad \{\mathbf{S}\} = \begin{bmatrix}S_{s4} & 0 & 0\\ 0 & S_{s5} & 0\\ 0 & 0 & S_{s5}\end{bmatrix}$$
$$S_{11} = 1/E_1,\quad S_{22} = 1/E_2,\quad S_{12} = -\nu_{21}/E_1,\quad S_{23} = -\nu_{32}/E_2$$
$$S_{s4} = 1/2G_{23} = S_{22} - S_{23},\quad S_{s5} = 1/2G_{12} \tag{A.14}$$

Vectors $\boldsymbol{\sigma}, \boldsymbol{\tau}, \boldsymbol{\varepsilon}, \boldsymbol{\delta}$ are defined in Eqns. $(A.3)_{1\text{-}4}$. Matrices $\mathbf{S}, \{\mathbf{S}\}$ are elastic compliance matrices corresponding to the normal/shear strains for a homogeneous monotropic material.

Unconjugated standard constitutive equations of the linear elasticity of a homogenized UFRT composite have the following form:

$$\boldsymbol{\varepsilon}_{\mathrm{s}} = \{\mathbf{S}_{\mathrm{s}}\}\boldsymbol{\sigma}_{\mathrm{s}}\,,\quad \boldsymbol{\varepsilon}_{\mathrm{b}} = \{\mathbf{S}_{\mathrm{b}}\}\boldsymbol{\sigma}_{\mathrm{b}} \tag{A.15}$$

where

$$\boldsymbol{\varepsilon}_{\mathrm{s}} = (\mathbf{I}-\mathbf{B})\boldsymbol{\varepsilon}\ ,\ \ \boldsymbol{\sigma}_{\mathrm{s}} = (\mathbf{I}-\mathbf{A})\boldsymbol{\sigma}\ ,\ \ \boldsymbol{\varepsilon}_{\mathrm{b}} = \mathbf{B}\boldsymbol{\varepsilon}\ ,\ \ \boldsymbol{\sigma}_{\mathrm{b}} = \mathbf{A}\boldsymbol{\sigma}$$
$$\{\mathbf{S}_{\mathrm{s}}\} = \mathrm{diag}\,(S_{\mathrm{s}1}, S_{\mathrm{s}2}, S_{\mathrm{s}2})\ ,\ \ \{\mathbf{S}_{\mathrm{b}}\} = \mathrm{diag}\,(S_{\mathrm{b}1}, S_{\mathrm{b}2}, S_{\mathrm{b}2})$$
$$\mathbf{I} = \mathrm{diag}\,(1,1,1)\ ,\ \ \mathbf{A} = \frac{1}{3}\begin{bmatrix}1 & 1/\lambda & 1/\lambda\\ \lambda & 1 & 1\\ \lambda & 1 & 1\end{bmatrix},\ \ \mathbf{B} = \begin{bmatrix}B_{11} & B_{12} & B_{13}\\ B_{21} & B_{22} & B_{23}\\ B_{31} & B_{32} & B_{33}\end{bmatrix} \tag{A.16}$$

with

$$\boldsymbol{\varepsilon} = \boldsymbol{\varepsilon}_{\mathrm{s}} + \boldsymbol{\varepsilon}_{\mathrm{b}}\ ,\ \ \boldsymbol{\sigma} = \boldsymbol{\sigma}_{\mathrm{s}} + \boldsymbol{\sigma}_{\mathrm{b}}$$
$$S_{\mathrm{s}1} = (1+\nu_{21}\lambda)/E_1\ ,\ \ S_{\mathrm{s}2} = S_{\mathrm{s}4} = 1/2G_{23}$$
$$S_{\mathrm{b}1} = (1-2\nu_{21}\lambda)/E_1\ ,\ \ S_{\mathrm{b}2} = 1/3B_2 \tag{A.17}$$
$$\lambda = \nu_{12}/\nu_{32}\ ,\ \ \nu_{12} = \nu_{21}E_2/E_1$$

The following nomenclature and interpretation are introduced: $\boldsymbol{\varepsilon}_{\mathrm{s}}, \boldsymbol{\varepsilon}_{\mathrm{b}}, \boldsymbol{\sigma}_{\mathrm{s}}, \boldsymbol{\sigma}_{\mathrm{b}}$ – vectors of the elastic quasi-shear/quasi-bulk strains/stresses in a monotropic material, $\{\mathbf{S}_{\mathrm{s}}\}, \{\mathbf{S}_{\mathrm{b}}\}$ – elastic quasi-shear/quasi-bulk compliance matrices describing a monotropic material, $\mathbf{A}, \mathbf{B}$ – transformation matrices.

Unconjugated standard constitutive equations of the linear elasticity and viscoelasticity of a UFRT composite have the following form:

$$\boldsymbol{\varepsilon}_{\mathrm{s}}(t) = \{\tilde{\mathbf{S}}_{\mathrm{s}}(t)\} \otimes \boldsymbol{\sigma}_{\mathrm{s}}(t)\ ,\ \ \boldsymbol{\varepsilon}_{\mathrm{b}}(t) = \{\mathbf{S}_{\mathrm{b}}\}\boldsymbol{\sigma}_{\mathrm{b}}(t)$$
$$\boldsymbol{\delta}(t) = \{\tilde{\mathbf{S}}(t)\} \otimes \boldsymbol{\tau}(t) \tag{A.18}$$

for time variable $t \geq 0$, with

$$\{\tilde{\mathbf{S}}_{\mathrm{s}}(t)\} = \mathrm{diag}[\tilde{S}_{\mathrm{s}1}(t), \tilde{S}_{\mathrm{s}4}(t), \tilde{S}_{\mathrm{s}4}(t)]\ ,$$
$$\{\tilde{\mathbf{S}}(\boldsymbol{t})\} = \mathrm{diag}[\tilde{S}_{\mathrm{s}4}(t), \tilde{S}_{\mathrm{s}5}(t), \tilde{S}_{\mathrm{s}5}(t)]$$
$$\tilde{S}_{\mathrm{s}j}(t) = S_{\mathrm{s}j}\left[1 + c_j \int_0^t \Phi(v)\, dv\right],\ \ j = 1,4,5$$
$$\Phi(t) = \frac{1}{T_{\mathrm{c}}}\int_0^{\infty} \exp\left(-\frac{ut}{T_{\mathrm{c}}}\right) u\, L(u)\, du$$
$$L(u) = \frac{\sin \pi r}{\pi u}\frac{u^r}{1+2u^r\cos \pi r + u^{2r}}\ ,\ \ 0 < r < 1 \tag{A.19}$$

The nomenclature and interpretation are as follows: $L(u)$ – function defining the Mittag-Leffler fractional exponential function in an integral form, r – fraction defining the Mittag-Leffler fractional exponential function, T_{c} – retardation time, $\Phi(t)$ – generic function for shear stresses (Mittag-Leffler fractional exponential function), $\{\tilde{\mathbf{S}}_{\mathrm{s}}(t)\}$ – elastic-viscoelastic quasi-shear compliance matrix, $\{\tilde{\mathbf{S}}(t)\}$ – elastic-viscoelastic shear compliance matrix, c_1, c_4, c_5 – long-term creep coefficients, $\otimes$ – convolution product operator.

The first equation contained in matrix equation $(A.18)_1$ is

$$\varepsilon_{\mathrm{s}1}(t) = \tilde{S}_{\mathrm{s}1}(t) \otimes \sigma_{\mathrm{s}1}(t)\ ,\ \ \tilde{S}_{\mathrm{s}1}(t) = S_{\mathrm{s}1}\left[1 + c_1 \int_0^t \Phi(v)\, dv\right] \tag{A.20}$$

The steady-state (harmonic) elastic-viscoelastic response in strain to the harmonic stress programme is

$$\varepsilon^*_{\mathrm{s}1}(t) = S_{\mathrm{s}1}\left[1 + c_1 \int_0^{\infty} \exp(-\mathrm{i}\omega v)\, \Phi(v)\, dv\right]\sigma^*_{\mathrm{s}1}(t) = S^*_{\mathrm{s}1}(\omega)\, \sigma^*_{\mathrm{s}1}(t) \tag{A.21}$$

where

$$S^*_{\mathrm{s}1}(\omega) = S_{\mathrm{s}1}\left[1 + c_1\, \overline{\Phi}(\mathrm{i}\omega)\right] = S_{\mathrm{s}1}\left[1 + c_1 \frac{1}{1+(\mathrm{i}\omega T_{\mathrm{c}})^r}\right]$$
$$= S'_{\mathrm{s}1}(\omega) + \mathrm{i}S''_{\mathrm{s}1}(\omega)$$
$$S'_{\mathrm{s}1}(\omega) = S_{\mathrm{s}1}\left[1 + c_1 \frac{1 + (\omega T_{\mathrm{c}})^r \cos(\pi r/2)}{1 + 2(\omega T_{\mathrm{c}})^r \cos(\pi r/2) + (\omega T_{\mathrm{c}})^{2r}}\right]$$
$$S''_{\mathrm{s}1}(\omega) = -S_{\mathrm{s}1} c_1 \frac{(\omega T_{\mathrm{c}})^r \sin(\pi r/2)}{1 + 2(\omega T_{\mathrm{c}})^r \cos(\pi r/2) + (\omega T_{\mathrm{c}})^{2r}} \tag{A.22}$$

with the following interpretation and nomenclature: $S^*_{\mathrm{s}1}(\omega)$ – first complex quasi-shear compliance, $S'_{\mathrm{s}1}(\omega)$ – first quasi-shear storage compliance, $S''_{\mathrm{s}1}(\omega)$ – first quasi-shear loss compliance.

Unconjugated inverse constitutive equations of the linear elasticity and viscoelasticity of a UFRT composite have the following form:

$$\boldsymbol{\sigma}_{\mathrm{s}}(t) = \{\tilde{\mathbf{C}}_{\mathrm{s}}(t)\} \otimes \boldsymbol{\varepsilon}_{\mathrm{s}}(t)\ ,\ \ \boldsymbol{\sigma}_{\mathrm{b}}(t) = \{\mathbf{C}_{\mathrm{b}}\}\boldsymbol{\varepsilon}_{\mathrm{b}}(t)$$
$$\boldsymbol{\tau}(t) = \{\tilde{\mathbf{C}}(t)\} \otimes \boldsymbol{\delta}(t) \tag{A.23}$$

for time variable $t \geq 0$, with

$$\{\tilde{\mathbf{C}}_{\mathrm{s}}(t)\} = \mathrm{diag}[\tilde{C}_{\mathrm{s}1}(t), \tilde{C}_{\mathrm{s}4}(t), \tilde{C}_{\mathrm{s}4}(t)]\ ,$$
$$\{\tilde{\mathbf{C}}(\boldsymbol{t})\} = \mathrm{diag}[\tilde{C}_{\mathrm{s}4}(t), \tilde{C}_{\mathrm{s}5}(t), \tilde{C}_{\mathrm{s}5}(t)]$$
$$\tilde{C}_{\mathrm{s}j}(t) = C_{\mathrm{s}j}\left[1 - d_j \int_0^t \Psi_j(v)\, dv\right],\ \ j = 1,4,5$$
$$\Psi_j(t) = \frac{1}{T_{d_j}}\int_0^{\infty} \exp\left(-\frac{ut}{T_{d_j}}\right) u\, L(u)\, du\ ,\ \ j = 1,4,5$$
$$d_j = \frac{c_j}{1+c_j}\ ,\ \ T_{d_j} = T_{\mathrm{c}} \exp\left(\frac{1}{r}\ln\frac{1}{1+c_j}\right)\ ,\ \ j = 1,4,5 \tag{A.24}$$

and the following nomenclature and interpretation: T_{d_j} – j-th relaxation time, $\Psi_j(t)$ – j-th shear strain generic function, $\{\tilde{\mathbf{C}}_{\mathrm{s}}(t)\}$ – elastic-viscoelastic quasi-shear stiffness matrix, $\{\tilde{\mathbf{C}}(t)\}$ – elastic-viscoelastic shear stiffness matrix, d_1, d_4, d_5 – long-term relaxation coefficients. Viscoelastic parameters d_j, T_{d_j}, $j = 1,4,5$, are expressed in terms of previous viscoelastic parameters c_j, T_{c}, $j = 1,4,5$, as specified in Eqns. $(A.24)_{5,6}$.

REFERENCES

[1] Klasztorny M., Nycz D.B., Modelling of linear elasticity and viscoelasticity of thermosets and unidirectional glass fibre--reinforced thermoset-matrix composites – Part 1: Theory of modelling, Composites Theory and Practice 2022, 22, 1, 3-15.

[2] Wilczynski A.P., A basic theory of reinforcement for unidirectional fibrous composites, Composites Science and Technology 1990, 38(4), 327-337, DOI: 10.1016/0266-3538 (90)90019-2.

[3] Wilczynski A.P., Lewinski J., Predicting the properties of unidirectional fibrous composites with monotropic reinforcement, Composites Science and Technology 1995, 55(2), 139-143, DOI: 10.1016/0266-3538(95)00090-9.

[4] Klasztorny M., Konderla P., Piekarski R., An exact stiffness theory for unidirectional xFRP composites, Mechanics of

Composite Materials 2009, 45(1), 77-104, DOI: 10.1007/s11029-009-9064-y.

[5] PN-EN ISO 527-1:1998. Plastics. Determination of mechanical properties in static tension. General rules [in Polish].

[6] PN-EN ISO 527-5:2000. Plastics. Determination of mechanical properties in static tension. Testing conditions for polymer-matrix composites reinforced with unidirectional fibres [in Polish].

[7] PN-EN ISO 14126:2002. Fibre-reinforced plastic composites. Determination of properties at in-plane compression [in Polish].

[8] ASTM D 5379/D 5379M-98. Standard Test Method for Shear Properties of Composite Materials by the V-Notched Beam Method.

[9] PN-ISO 2602:1994. Statistical interpretation of test results. Estimation of mean value. Confidence interval [in Polish].

[10] Klasztorny M., Kiczko A., Nycz D.B., Identification tests on UFRT composite at normal conditions [in Polish], Report No. WAT/WME/4/2014, Research Project No. PBS1/B2/6/2013, Military University of Technology, Warsaw, Poland.

[11] Szmelter J., Computational Methods in Mechanics [in Polish], PWN Press, Warsaw 1980.

[12] Gauss-Legendre quadrature weighs and nodes. Engineering Fundamentals, http://www.efunda.com, access 05/15/2021.

